

Regular Article

Study of Schiff-Base-Derived with Dioxygenated Rings and Nitrogen Heterocycle as Potential β -Ketoacyl-acyl Carrier Protein Synthase III (FabH) Inhibitors

Yang Zhou,^{a,#} Yu-Shun Yang,^{a,#} Xiao-Da Song,^b Liang Lu,^a and Hai-Liang Zhu^{*,a}

^aState Key Laboratory of Pharmaceutical Biotechnology, Nanjing University; Nanjing 210023, China; and ^bSchool of Life Science and Technology, China Pharmaceutical University; Nanjing, 210009, China.

Received September 28, 2016; accepted November 23, 2016

Fatty acid synthesis (FAS) is an essential metabolism during the whole growth and development process of the bacterial. Several key enzymes which involved in this biosynthetic pathway have been considered as useful targets for the development of new antibacterial agents. Among them, β -ketoacyl-acyl carrier protein synthase III (FabH) is the most magnetic target, since it is central to the initiation of fatty acid biosynthesis and is highly conserved of both Gram-positive and Gram-negative bacteria. Following the previous researches, Schiff-based derivatives with dioxygenated rings and *N*-heterocycle were synthesized in succession, and their biological activities as potential FabH inhibitors were evaluated in this paper. Among these 15 compounds, compound 2E exhibited the best antibacterial activities with minimum inhibitory concentration (MIC) values 1.56–3.13 mg/mL against the tested bacterial strains and showed the most powerful *Escherichia coli* (*E. coli*) FabH inhibitory activities with IC₅₀ of 2.1 μ M. Also the conceivable binding conformation of placing compound 2E into the *E. coli* FabH active site was affirmed docking simulation.

Key words antibacterial-agent; dioxygenated-ring; *N*-heterocycle; β -ketoacyl-acyl carrier protein synthase III (FabH); FabH inhibitor

A number of antibiotics have been invented and applied to against diseases after Fleming found penicillin in 1928 and Flory used penicillin in the treatment of infectious diseases in 1940.¹⁾ Antibiotics have become one of the greatest achievements in the field of medicine and made great contribution for health of people in 20th Century. But many pathogenic bacteria showed drug resistances to antibiotics for the abuse used of antibiotics. The occurrence of drug resistance and the propagation speed of pathogenic bacteria are eye-popping.²⁾ So looking for new antibacterial targets and develop new antibacterial agents is urgent. Fatty acid synthesis (FAS) play an effective role in the metabolic process of most organisms. Comparing the FAS I (exist in Mammals and yeast),^{3–5)} FAS II exist in bacteria and plants, form by a series of separated small proteins. Each step of the FAS is catalyzed by specific monofunctional enzyme independent.^{6–8)} So developing of new antibacterial agents targeting one or several monofunctional enzymes in bacterial fatty acid synthesis become quite feasible.^{9,10)}

Among all enzymes of bacterial fatty acid synthesis, β -ketoacyl-acyl carrier protein (ACP) synthase III (FabH) shows some special characteristics¹¹⁾: (1) It catalyzes the starting step of FAS rotate; (2) FabH can be inhibited by the final product Palmitoyl-ACP and the whole loop terminates, so it plays a key role in regulation of FAS; (3) FabH has higher substrate specificity. The substrate of the FabH is only acetyl CoA, while both FabB and FabF use Acyl-ACP as their substrate; (4) FabH is prevalently existed in a large number of clinical pathogens, such as Gram-positive bacteria, Gram-negative bacteria, chlamydia, anaerobic bacteria, mycobacteria. FabH is also essential in their survival, while some

enzymes, for example, FabA, FabB, FabI are not found in all pathogens.¹²⁾

The notable features of the FabH have attracted a great number of researchers and many pioneer studies focusing on FabH have been reported.^{13–15)} FabH shows high conserved on gene sequences and three-dimensional structures of Gram-positive bacteria and Gram-negative bacteria, while any homologous proteins cannot be found in human. More importantly, amino acid residues at FabH active sites between Gram-positive and Gram-negative bacteria were no essential differences. FabH has been identified is the key target enzyme in the fatty acid synthesis of bacteria, and can be chosen as the new target for developing broad-spectrum antibiotics.^{16–18)}

Many research groups including our group devoted to investigating antibacterial with FabH as target, and some potential FabH inhibitors with high antibacterial activities have been exploited^{19–24)} (Fig. 1).

Four novel Schiff bases derived from YKAs3003 that retained cyclohexylamine moiety as skeleton structure were designed in the previous studies. Among them, seven-membered ring was taken as the most appropriate structure for developing new FabH inhibitor *via* receptor-oriented pharmacophore model and docking. A series of compounds were synthesized and evaluated against different bacterial and tested their *Escherichia coli* (*E. coli*) FabH inhibitory activities. Compound **10** containing 16 aliphatic substituents was found as the most potent *E. coli* FabH inhibitory activity with an IC₅₀ value of 1.6 μ M. During this process of developing antibiotic agents, we also found that the nitrogen heterocycle replacing at the right side showed better antibacterial activity than benzene ring, it could be another strategy to explore better antibacterial agents.²⁵⁾ We synthesize and evaluate a series of Schiff base with nitrogen heterocycle substitute and dioxygenated seven-

[#]These authors contributed equally to this work.

* To whom correspondence should be addressed. e-mail: zhuhl@nju.edu.cn

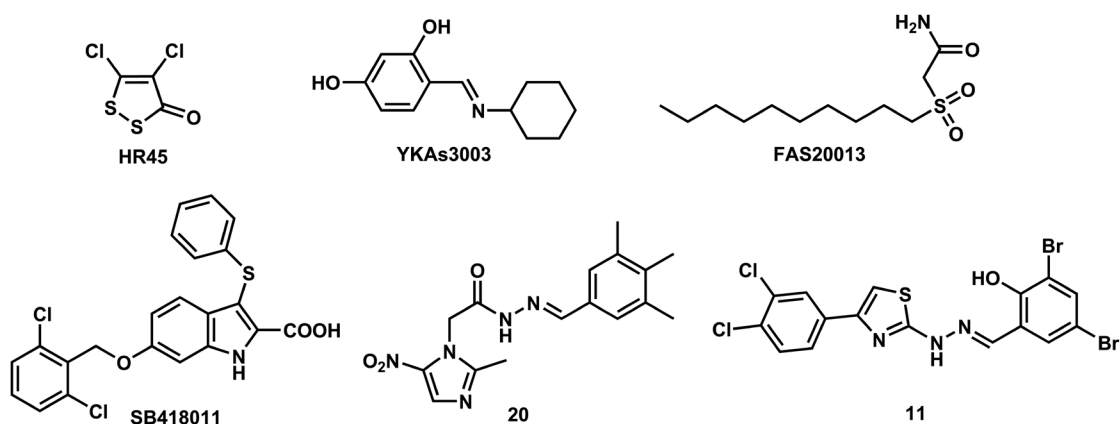


Fig. 1. Several Reported Antibacterial Agents Targeting FabH

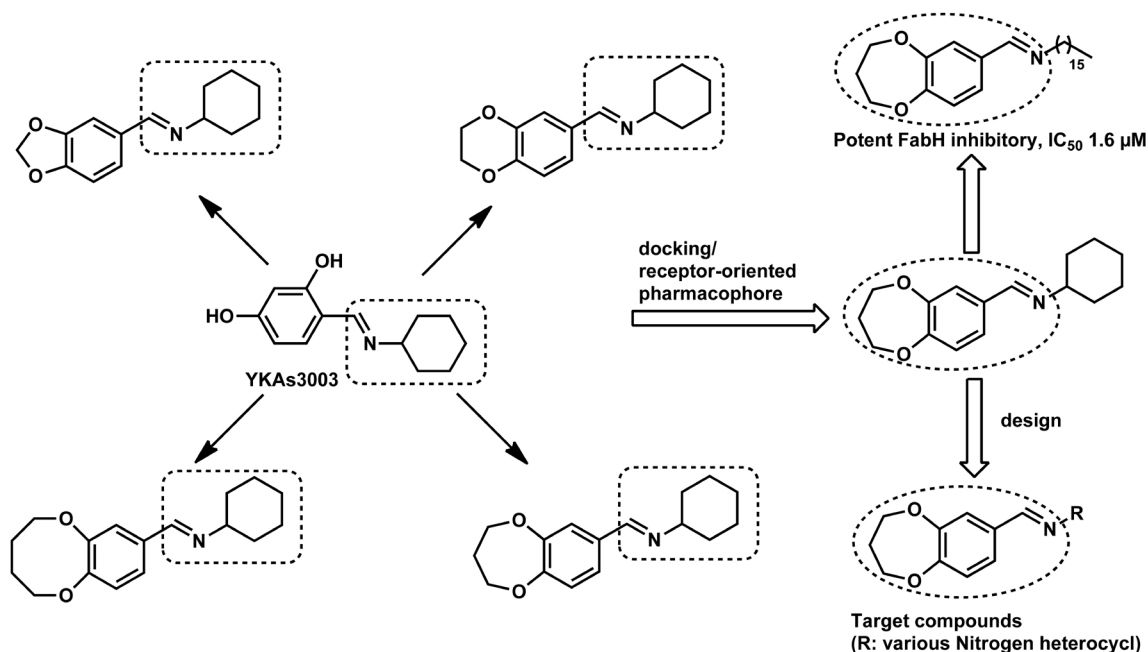


Fig. 2. Design Strategy

A lead compound (YKAs3003) initiates a series of novel antibiotic agents with nitrogen heterocycle.

membered fuse ring, and investigate their biological activities in this paper. The whole design strategy was showed in Fig. 2.

Results and Discussion

Chemistry The synthesis of targeted compounds **2A–O** was presented in Fig. 3. The synthesis of intermediate aldehyde **1** was similar to previous article.²⁵⁾ For developing more effective antibiotics agents and discussing the different trends in structure–activity relationships (SARs) of the designed compounds handily, the substituents on the right hand were divided into two parts, one with heterocyclic methanamine group, the other heterocycle amine. Dehydration reaction by different amines and intermediate aldehyde **1** produced the final designed analogues. The products **2A–O** were obtained with 77–93% yields *via* flash chromatography. The structures of these compounds were fully characterized by spectroscopic methods and elemental analysis.

Biological Activity Two Gram-negative bacterial strains, *E. coli* and *P. fluorescence*, and the two Gram-positive bacte-

rial strains, *B. subtilis* and *S. aureus*, were used to evaluate the antibacterial activity of all compounds (**2A–O**), with the 3-(4,5-dimethylthiazole-2-yl)-2,5-diphenyltetrazolium bromide (MTT) assay. The minimum inhibitory concentrations (MIC) of these compounds against these bacteria were presented in Table 1. As the positive control, kanamycin B was also evaluated its antibacterial activity in the same condition with other synthesized compounds (**2A–O**).

For discussing the SARs of these compounds, we divided the compounds into two groups: compounds (**2A–D**) which bear heterocyclic methanamine and compounds (**2E–O**) which bear heterocyclic amine. The methylene between imine and the heterocyclic show no effect on the activities, which meant length of the linker between N atom and *N*-heterocyclic (with none or one-carbon-atom gaps) was not the quite important factor of the antibacterial activities. However, Schiff-base compounds **2A**, **F**, **G** with lower predicted lipophilicity ($AlogP < 2$) values exhibited poor activities. Compounds with substituent groups on the heterocyclic (**2D**, **E**, **J**, **K**, **M–O**)

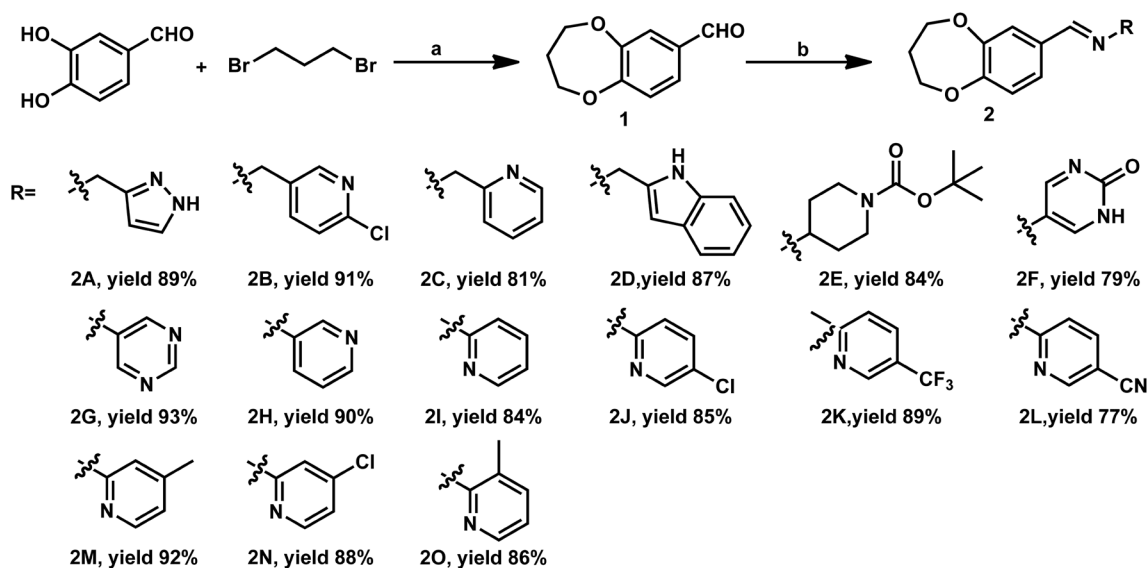


Fig. 3. General Synthesis of the Schiff Base Derivatives 2A–O

Reagents and conditions: a) Cs_2CO_3 , DMF, 70°C , overnight; b) R-NH_2 , EtOH, RT, overnight.

Table 1. Antibacterial Activity of Synthetic Compounds

Compd. ^{a)}	$A \log P^b)$	Minimum inhibitory concentrations [$\mu\text{g/mL}$]			
		Gram-negative		Gram-positive	
		<i>E. coli</i>	<i>P. aeruginosa</i>	<i>B. subtilis</i>	<i>S. aureus</i>
2A	1.940	50	>100	>100	>100
2B	2.986	25	50	>100	>100
2C	2.346	25	50	50	50
2D	3.004	6.25	12.5	25	25
2E	2.642	1.56	1.56	3.13	3.13
2F	0.841	50	25	>100	>100
2G	1.496	>100	>100	>100	>100
2H	2.124	25	12.5	25	50
2I	2.663	50	50	>100	>100
2J	3.327	6.25	12.5	25	50
2K	3.605	6.25	3.13	12.5	6.25
2L	2.542	12.5	12.5	12.5	25
2M	3.149	6.25	12.5	6.25	12.5
2N	3.327	12.5	6.25	25	12.5
2O	3.149	6.25	6.25	12.5	25
Kanamycin B	-7.144	3.13	3.13	1.56	1.56

a) The compounds tested for antibacterial activity are consistent with the description in Experimental. b) Calculated with discovery studio 3.1.²⁶⁾

seemed to enhance the antibacterial activities than others with no substituent groups (2B, C, H, I). Compound 2D represented an exception, probably because the benzene of the 3H-indole could make up for the loss of substituent groups on N-heterocyclic caused by the length of the linker. No significant difference could be found between electron withdrawing substituents (2D, J–L, N) or electron-donating substituents (2M, O) on the N-heterocyclic. The position of the substituents at 4- or 5-pyridine didn't obviously enhance the antibacterial activities. Regarding the substituent of pyridine, trifluoromethyl did better than other moieties (2K). The last noticeable discovery from compound 2E with *tert*-butyl piperidine carboxylate was the highest activity, that the piperidine ring replacing another N-heterocyclic might provide one more tactics to develop better antibacterial agents.

Then we evaluated the *E. coli* FabH inhibition of these synthetic compounds with potential antibacterial activities (2D, E, H, J–O), and the results were performed in Table 2. All compounds presented potent *E. coli* FabH inhibition, and the compound 2E with *tert*-butyl piperidine carboxylate showed the best activity against *E. coli* FabH with the IC_{50} value of $2.1 \mu\text{M}$. This result indicated the potent antibacterial activities of compound 2E being the most potent FabH inhibitor. Compound 2K with trifluoromethyl substituent of the pyridine also showed higher activities than others compounds. This due to the trifluoromethyl not only caused the compound with highest $A \log P$ value ($A \log P$ 3.605) but also was a quite important substituent group in drug metabolism. Since the molecular polar surface area (PSA) is a considerable parameter in predicting drug transport, we calculated PSA in Table

Table 2. *E. coli* FabH Inhibitory Activity of Synthesized Compounds

Compd. ^{a)}	<i>E. coli</i> FabH IC ₅₀ [μ M]	PSA ^{b)} [\AA^2]	Hemolysis LC ^{c)} [mg/mL]	Cytotoxicity IC ₅₀ [μ M]
2D	6.7	40.41	>10	148.7
2E	2.1	58.77	>10	189.5
2H	14.5	40.44	>10	138.1
2J	12.8	40.44	>10	178.4
2K	3.8	40.44	>10	198.6
2L	9.9	63.38	>10	154.9
2M	12.3	40.44	>10	201.3
2N	15.1	40.44	>10	180.4
2O	7.4	40.44	>10	125.6

a) The compounds tested for antibacterial activity are consistent with the description in Experimental. b) The PSA was calculated by discovery studio 3.1.²⁶⁾ c) Lytic concentration 30%.

2 too, which would relate the the binding affinity and the cell permeability of FabH inhibitors.²⁷⁾ The molecular PSA values of these compounds were in the range of 40–64 \AA^2 , and therefore, this molecular property cannot significantly account for the results obtained. To sum up, the results of the *E. coli* FabH inhibitory activity of the test compounds described above extensively conformed to the SARs of their antibacterial activities. This exhibited that the efficient antibacterial activities of these compounds might be from their FabH inhibitory activities.

The hemolytic activities of these selected compounds were observed. And the cytotoxic activities were also tested by mouse embryonic fibroblast cell line (NIH-3T3) using the MTT assay as well.²⁸⁾ These results were summarized in Table 2.

All the compounds displayed low hemolytic activities. Besides, the cytotoxicity assay determined the selectivity of our compounds for bacterial over mammalian cells. All these data suggested that the compounds with potent inhibitory activities were low toxic.

The *E. coli* FabH inhibitory activity of compound **2E** is lower than compound **10**, but the MIC values of compound **2E** and compound **10** are both described as 1.56 μ g/mL against *E. coli* in the same experimental condition. For deeper comparison of the biological activities between compound **10** and compound **2E**, we have reset the gradients of these two compounds from 0 to 1.6 μ g/mL per 0.1 μ g/mL. Then the results showed MIC of compound **2E** and compound **10** were 1.1 and 1.5 μ g/mL, respectively. We did not raise this detailed data because the absorption, distribution, metabolism, excretion and toxicity (ADMET) properties were more directly to indicate the advantages of compound **2E** in this manuscript. The MIC value in deeper comparison actually reflect the same point. The *AlogP* value of compound **10** was 8.501, whereas that of compound **2E** was 2.642. According to Lipinski's Rule of Five, the range of *AlogP* values for medicine should be -0.5 – 5.6 . Thus, even compound **10** was slightly better than compound **2E** in *E. coli* FabH inhibitory activity, when applied to practice, compound **2E** could be more potential.

Molecular docking of the most active compound **2E** and *E. coli* FabH was displayed for demonstrating the interaction binding mode between the target protein and small molecules, which used the he *E. coli* FabH–CoA complex structure (PDB: 1HNJ) as binding model.¹³⁾ The accompanying results were shown in Fig. 4, composed of two interaction maps. The docking study was performed using the CDocker protocol.²⁶⁾

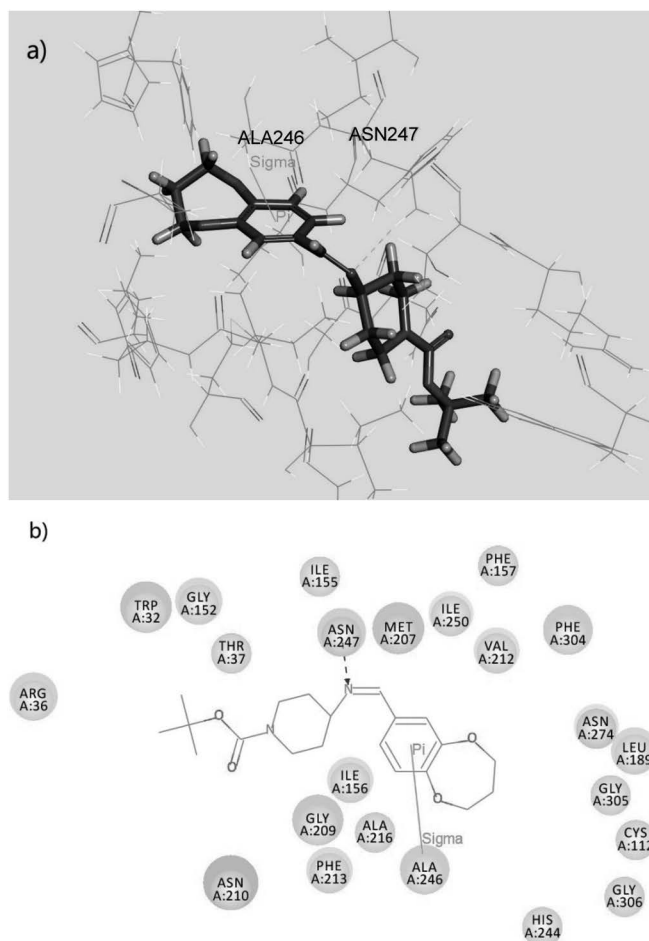


Fig. 4. (a) 3D Model of the Interaction between Compound **2E** and 1HNJ Binding Site; (b) 2D Molecular Docking Model of Compound **2E** with 1HNJ

The H-bond was displayed as dotted line and the amino acid it acts on is labeled. The π -sigma interaction was shown as straight line with correlated amino acid labeled.

The three dimensional (3D) optimal conformation and the 2D diagram interacting with the FabH active site was presented in Figs. 4a and 4b, respectively. The main chain of ASN147 forms hydrogen bond (NH–N, 2.34 \AA , 169.512 $^\circ$) with one nitrogen atom of compound **2E** while ALA246 participate in a π -sigma interaction (2.81 \AA) with the benzene ring of compound **2E**.

These interactions were critical for the stabilization of the

binding mode. Comparing with the original crystal conformation of substrate malonyl-CoA, compound **2E** indicated more powerful interactions with the active site. Hence, compound **2E** could be considered as a potential inhibitor of *E. coli* FabH with potent antibacterial activity.

Conclusion

In this paper, 15 novel Schiff base with different *N*-heterocyclic were synthesized and their antibacterial activities against *E. coli* FabH were evaluated firstly. Within our research, certain compounds (**2D**, **E**, **H**, **J–O**) showed anti-Gram-negative bacteria activities. Compound **2E** exhibited the best antibacterial activity with MIC values of 1.56–3.13 mg/mL against the tested bacterial strains and presented the most potent *E. coli* FabH inhibitory activity with IC₅₀ of 2.1 μM. Initiatory structure–activity relationships and molecular modeling study provided further insight into interactions between the enzyme and its ligands. This study showed that **2E** was a novel compound that could be potent antimicrobial inhibitor of FabH and provide useful advice for the designed of *E. coli* FabH inhibitors as an antibacterial agents. Moreover, developing novel compounds bearing similar structures of compound **2E** will be investigated in future studies.

Experimental

Chemistry

General

All chemicals (reagent grade) were purchased from Sigma-Aldrich. Separation of the compounds by column chromatography was carried out with silica gel 60 (200–300 mesh ASTM, Merck, Germany). The quantity of silica gel used was 50–100 times the weight charged on the column. Then, the eluates were monitored using TLC. Melting points (mp) were determined on a XT4 MP apparatus (Taike Corp., Beijing, China). Electrospray ionization (ESI) MS were obtained on a Mariner System 5304 mass spectrometer, and ¹H- and ¹³C-NMR spectra were recorded on a Bruker DPX 400 spectrometer. Elemental analyses were performed on a Heraeus CHN-O-Rapid instrument and were within ±0.4% of the theoretical values.

3,4-Dihydro-2*H*-benzo[*b*][1,4]dioxepine-7-carbaldehyde (**1**)

An 25-mL round flask was charged with 3,4-dihydroxybenzaldehyde (0.716 g, 5.20 mmol, 1.0 equiv.), Cs₂CO₃ (3.38 g, 10.4 mmol, 2.0 equiv.) and *N,N*-dimethylformamide (DMF) (8 mL). 1,3-Dibromopropane (2.10 g, 10.4 mmol, 2.0 equiv.) was added. The reaction mixture was refluxed at 70°C overnight. After cooled to the room temperature (RT), the reaction solution was filtered through a short pad of Celite and the filtrate was concentrated under reduced pressure. The residue was purified by column chromatography on silica gel to give compound **1** as a colorless oil. Yield: 88%. *R*_f=0.6 (4:1 hexane–EtOAc). ¹H-NMR (400 MHz, CDCl₃) δ: 9.85 (s, 1H), 7.47 (dd, *J*=7.2, 1.8 Hz, 2H), 7.06 (m, 1H), 4.36 (m, 2H), 4.30 (t, *J*=5.9 Hz, 2H), 2.26 (m, 2H). ¹³C-NMR (100 MHz, CDCl₃) δ: 190.54, 156.44, 151.01, 131.93, 125.36, 122.74, 121.79, 70.28, 70.15, 30.73. MS (ESI): *m/z* 179.2 [M+H]⁺. *Anal.* Calcd for C₁₀H₁₀O₃: C 67.41, H 5.66, O 26.94; Found: C 67.32, H 5.68, O 26.96.

Compounds 2 Compound **1** (535 mg, 3.00 mmol, 1 equiv.) was dissolved in MeOH (3 mL). The corresponding amine (3.6 mmol) was added. The reaction mixture was stirred at RT

for overnight. The solvent was removed under reduced pressure. The residue was purified by column chromatography (neutral Al₂O₃, EtOAc/hexane) to give pure compound **2**.

(*E*)-*N*-((3,4-Dihydro-2*H*-benzo[*b*][1,4]dioxepin-7-yl)-methylene)-1-(1*H*-pyrazol-3-yl)methanamine (**2A**)

White solid; yield: 89%. *R*_f=0.5 (4:1 hexane–EtOAc); mp: 105.2–105.8°C. ¹H-NMR (400 MHz, dimethyl sulfoxide (DMSO)-*d*₆) δ: 8.31 (s, 2H), 8.05 (s, 1H), 7.14 (d, *J*=2.0 Hz, 1H), 7.07 (dd, *J*=8.3, 2.0 Hz, 1H), 6.69 (d, *J*=8.3 Hz, 1H), 4.80 (s, 2H), 4.27 (m, 4H), 2.21 (m, 2H); ¹³C-NMR (100 MHz, DMSO-*d*₆) δ: 158.31, 157.08, 153.24, 139.37, 128.63, 125.56, 122.18, 121.74, 70.42, 70.39, 64.97, 31.59. MS (ESI): *m/z* 258.1 [M+H]⁺. *Anal.* Calcd for C₁₄H₁₅N₃O₂: C 65.35, H 5.88, N 16.33, O 12.44; Found: C 65.42, H 5.83, N 16.36, O 12.49.

(*E*)-*N*-((3,4-Dihydro-2*H*-benzo[*b*][1,4]dioxepin-7-yl)-methylene)-1-(3*H*-indol-2-yl)methanamine (**2B**)

White solid; yield: 91%. *R*_f=0.5 (4:1 hexane–EtOAc); mp: 145.7–146.3°C. ¹H-NMR (400 MHz, DMSO-*d*₆) δ: 8.24 (d, *J*=12.8 Hz, 2H), 7.87 (d, *J*=7.7 Hz, 1H), 7.55 (d, *J*=6.3 Hz, 2H), 7.48 (d, *J*=10.6 Hz, 1H), 7.40 (t, *J*=7.3 Hz, 1H), 7.23 (t, *J*=7.3 Hz, 1H), 6.99 (m, 2H), 4.25 (m, 4H), 3.16 (s, 2H), 2.21 (m, 2H); ¹³C-NMR (100 MHz, DMSO-*d*₆) δ: 160.45, 153.38, 151.21, 136.36, 131.93, 127.67, 123.49, 122.33, 121.91, 121.64, 121.26, 119.26, 119.08, 114.09, 111.24, 61.95, 36.52, 31.05. MS (ESI): *m/z* 307.1 [M+H]⁺. *Anal.* Calcd for C₁₉H₁₈N₂O₂: C 74.49, H 5.92, N 9.14, O 10.44; Found: C 71.53, H 5.94, N 9.15, O 10.48.

(*E*)-*N*-((3,4-Dihydro-2*H*-benzo[*b*][1,4]dioxepin-7-yl)-methylene)-1-(pyridin-3-yl)methanamine (**2C**)

White solid; yield: 81%. *R*_f=0.5 (4:1 hexane–EtOAc); mp: 145.7–146.3°C. ¹H-NMR (400 MHz, DMSO-*d*₆) δ: 8.59 (s, H), 8.50 (dd, *J*=7.7, 1.7 Hz, 1H), 8.45–8.40 (m, 1H), 8.01 (s, 1H), 7.52–7.43 (m, 1H), 7.37 (q, *J*=4.9 Hz, 1H), 7.00 (dd, *J*=22.5, 8.5 Hz, 1H), 4.76 (s, 2H), 4.23–4.08 (m, 4H), 2.12 (dt, *J*=10.2, 5.2 Hz, 2H). ¹³C-NMR (100 MHz, DMSO-*d*₆) δ: 161.85, 153.74, 150.63, 149.73, 148.71, 136.13, 128.80, 125.09, 123.84, 123.02, 122.21, 121.43, 70.88, 70.82, 61.49, 31.59. MS (ESI): *m/z* 269.3 [M+H]⁺. *Anal.* Calcd for C₁₆H₁₆N₂O₂: C 71.62, H 6.01, N 10.44, O 11.93; Found: C 71.57, H 5.99, N 10.49, O 11.91.

(*E*)-1-(6-Chloropyridin-3-yl)-*N*-((3,4-dihydro-2*H*-benzo[*b*][1,4]dioxepin-7-yl)methylene)methanamine (**2D**)

White solid; yield: 87%. *R*_f=0.5 (4:1 hexane–EtOAc); mp: 120.3–120.9°C. ¹H-NMR (400 MHz, DMSO-*d*₆) δ: 8.52 (s, 1H), 8.19 (d, *J*=2.3 Hz, 1H), 8.02 (d, *J*=8.2 Hz, 1H), 7.62 (d, *J*=8.3 Hz, 1H), 7.38 (d, *J*=8.0 Hz, 1H), 6.85 (s, 2H), 4.38 (s, 2H), 4.28 (dt, *J*=14.7, 5.7 Hz, 4H), 2.23 (m, 2H). ¹³C-NMR (100 MHz, DMSO-*d*₆) δ: 161.89, 154.38, 150.28, 149.72, 148.16, 136.36, 128.31, 125.05, 123.94, 123.11, 122.40, 121.28, 70.42, 70.38, 62.28, 31.29. MS (ESI): *m/z* 303.4 [M+H]⁺. *Anal.* Calcd for C₁₆H₁₅ClN₂O₂: C 63.47, H 4.99, Cl 11.71, N 9.25, O 10.57; Found: C 63.54, H 5.02, Cl 11.65, N 9.25, O 10.48.

(*E*)-*tert*-Butyl 4-((3,4-Dihydro-2*H*-benzo[*b*][1,4]dioxepin-7-yl)methyleneamino)piperidine-1-carboxylate (**2E**)

Brown solid; yield: 84%. *R*_f=0.6 (4:1 hexane–EtOAc); mp: 89.7–90.1°C. ¹H-NMR (400 MHz, DMSO-*d*₆) δ: 8.30 (s, 1H), 7.47 (s, 1H), 7.14 (d, *J*=8.2 Hz, 1H), 6.70 (d, *J*=16.3 Hz, 1H), 4.31–4.26 (m, 4H), 4.22 (dd, *J*=10.1, 4.2 Hz, 4H), 3.90 (d, *J*=12.9 Hz, 1H), 2.28 (m, 2H), 2.18 (dt, *J*=9.8, 3.7 Hz, 4H), 1.42 (s, 9H). ¹³C-NMR (100 MHz, DMSO-*d*₆) δ: 161.28, 157.48, 153.08, 151.13, 132.27, 123.32, 121.51, 121.08, 79.82, 70.43, 70.41, 69.79, 44.40, 31.54, 29.66, 24.82. MS (ESI): *m/z*

361.4 [M+H]⁺. *Anal.* Calcd for C₂₀H₂₈N₂O₄: C 66.64, H 7.83, N 7.77, O 17.76; Found: C 66.56, H 7.80, N 7.83, O 17.69.

(*E*)-5-((3,4-Dihydro-2*H*-benzo[*b*][1,4]dioxepin-7-yl)-methyleneamino)pyrimidin-2(1*H*)-one (**2F**)

White solid; yield 79%. *Rf*=0.3 (4:1 hexane–EtOAc); mp: 121.4–122.3°C. ¹H-NMR (400 MHz, DMSO-*d*₆) δ: 8.17 (s, 1H), 8.01 (s, 1H), 7.31 (d, *J*=7.0 Hz, 1H), 7.08 (d, *J*=8.0 Hz, 1H), 6.85 (s, 2H), 5.56 (d, *J*=7.0 Hz, 1H), 4.21 (dt, *J*=10.8, 5.6 Hz, 4H), 2.15 (dt, *J*=11.0, 5.6 Hz, 2H). ¹³C-NMR (100 MHz, DMSO-*d*₆) δ: 163.72, 158.81, 155.19, 154.24, 148.90, 132.39, 128.93, 124.08, 122.26, 121.65, 105.49, 70.87, 70.85, 31.55. MS (ESI): *m/z* 272.3 [M+H]⁺. *Anal.* Calcd for C₁₄H₁₃N₃O₃: C 61.99, H 4.83, N 15.49, O 17.69; Found: C 62.04, H 4.83, N 15.41, O 17.75.

(*E*)-*N*-((3,4-Dihydro-2*H*-benzo[*b*][1,4]dioxepin-7-yl)-methylene)pyrimidin-4-amine (**2G**)

White solid; yield: 93%. *Rf*=0.4 (4:1 hexane–EtOAc); mp: 143.7–144.5°C. ¹H-NMR (400 MHz, DMSO-*d*₆) δ: 8.61 (s, 1H), 8.32 (s, 1H), 8.03 (d, *J*=5.9 Hz, 1H), 7.46 (d, *J*=2.1 Hz, 1H), 7.35 (dd, *J*=8.3, 2.0 Hz, 1H), 6.98 (d, *J*=8.2 Hz, 1H), 6.40 (dd, *J*=5.9, 1.3 Hz, 1H), 4.24 (dt, *J*=11.6, 5.7 Hz, 4H), 2.23 (m, 2H). ¹³C-NMR (100 MHz, DMSO-*d*₆) δ: 167.20, 164.34, 158.36, 154.21, 143.07, 131.28, 129.20, 124.38, 122.20, 121.80, 115.01, 70.42, 70.38, 31.27. MS (ESI): *m/z* 256.1 [M+H]⁺. *Anal.* Calcd for C₁₄H₁₃N₃O₂: C 65.87, H 5.13, N 16.46, O 12.54; Found: C 65.91, H 5.10, N 14.48, O 12.59.

(*E*)-*N*-((3,4-Dihydro-2*H*-benzo[*b*][1,4]dioxepin-7-yl)-methylene)pyridin-3-amine (**2H**)

White solid; yield 90%. *Rf*=0.4 (4:1 hexane–EtOAc); mp: 135.9–136.4°C. ¹H-NMR (400 MHz, DMSO-*d*₆) δ: 8.58 (s, 1H), 8.46 (ddd, *J*=6.2, 3.6, 1.0 Hz, 2H), 7.67 (ddd, *J*=8.1, 2.6, 1.5 Hz, 1H), 7.59–7.52 (m, 2H), 7.48–7.39 (m, 1H), 7.13–7.06 (m, 1H), 4.22 (dt, *J*=13.1, 5.8 Hz, 4H), 2.20–2.12 (m, 2H). ¹³C-NMR (100 MHz, DMSO-*d*₆) δ: 162.13, 154.58, 151.41, 147.70, 147.31, 143.38, 131.70, 128.09, 124.84, 124.47, 122.38, 122.33, 70.92, 70.84, 31.44. MS (ESI): *m/z* 255.3 [M+H]⁺. *Anal.* Calcd for C₁₅H₁₄N₂O₃: C 70.85, H 5.55, N 11.02, O 12.58; Found: C 70.76, H 5.59, N 11.16, O 12.41.

(*E*)-*N*-((3,4-Dihydro-2*H*-benzo[*b*][1,4]dioxepin-7-yl)-methylene)pyridin-2-amine (**2I**)

White solid; yield: 84%. *Rf*=0.4 (4:1 hexane–EtOAc); mp: 145.3–145.7°C. ¹H-NMR (400 MHz, DMSO-*d*₆) δ: 9.01 (s, 1H), 8.39 (dd, *J*=8.3, 1.7 Hz, 1H), 7.53 (ddd, *J*=8.2, 5.9, 3.1 Hz, 1H), 7.36–7.26 (m, 2H), 7.19–7.11 (m, 1H), 7.08–6.94 (m, 1H), 6.89–6.81 (m, 1H), 4.23 (dd, *J*=11.0, 5.5 Hz, 4H), 2.17 (td, *J*=9.8, 5.5 Hz, 2H). ¹³C-NMR (100 MHz, DMSO-*d*₆) δ: 162.24, 156.68, 154.34, 151.47, 150.29, 145.68, 142.84, 137.90, 129.22, 127.22, 125.03, 122.97, 115.22, 70.92, 70.79, 30.95. MS (ESI): *m/z* 255.3 [M+H]⁺. *Anal.* Calcd for C₁₅H₁₄N₂O₃: C 70.85, H 5.55, N 11.02, O 12.58; Found: C 70.92, H 5.54, N 11.08, O 12.50.

(*E*)-5-Chloro-*N*-((3,4-dihydro-2*H*-benzo[*b*][1,4]dioxepin-7-yl)methylene)pyridin-2-amine (**2J**)

White solid; yield: 85%. *Rf*=0.4 (4:1 hexane–EtOAc); mp: 138.2–138.8°C. ¹H-NMR (400 MHz, DMSO-*d*₆) δ: 9.03 (s, 1H), 8.52 (d, *J*=2.6 Hz, 1H), 7.62 (dd, *J*=7.5, 1.7 Hz, 2H), 7.36 (d, *J*=8.5 Hz, 1H), 7.13–7.07 (m, 1H), 6.45 (dd, *J*=8.8, 0.6 Hz, 1H), 4.30–4.15 (m, 4H), 2.16 (dq, *J*=11.6, 5.9 Hz, 2H). ¹³C-NMR (100 MHz, DMSO-*d*₆) δ: 162.63, 158.98, 151.42, 147.68, 146.11, 138.75, 137.17, 131.25, 125.53, 122.77, 121.17, 117.79, 70.87, 70.83, 31.35. MS (ESI): *m/z* 289.2 [M+H]⁺. *Anal.*

Calcd for C₁₅H₁₃ClN₂O₂: C 62.40, H 4.54, Cl 12.28, N 9.70, O 11.08; Found: C 62.47, H 4.55, Cl 12.34, N 9.62, O 11.08.

(*E*)-*N*-((3,4-Dihydro-2*H*-benzo[*b*][1,4]dioxepin-7-yl)-methylene)-5-(trifluoromethyl)pyridin-2-amine (**2K**)

White solid; yield: 89%. *Rf*=0.5 (4:1 hexane–EtOAc); mp: 127.5–128.1°C. ¹H-NMR (400 MHz, DMSO-*d*₆) δ: 8.51 (s, 1H), 8.03–7.96 (m, 1H), 7.70 (dd, *J*=8.9, 2.4 Hz, 1H), 7.08–6.92 (m, 2H), 6.73 (d, *J*=8.9 Hz, 1H), 6.62 (dd, *J*=5.4, 1.7 Hz, 1H), 4.11 (dd, *J*=8.4, 5.3 Hz, 4H), 2.10 (dd, *J*=10.9, 5.5 Hz, 2H). ¹³C-NMR (100 MHz, DMSO-*d*₆) δ: 162.61, 159.95, 156.70, 151.26, 150.94, 146.17, 134.37, 132.28, 125.66, 122.98, 122.15, 120.13, 114.13, 70.82, 70.76, 31.96. MS (ESI): *m/z* 322.3 [M+H]⁺. *Anal.* Calcd for C₁₆H₁₃F₃N₂O₂: C 59.63, H 4.07, F 17.68, N 8.69, O 9.93; Found: C 59.68, H 4.09, F 17.53, N 8.73, O 9.89.

(*E*)-6-((3,4-Dihydro-2*H*-benzo[*b*][1,4]dioxepin-7-yl)-methyleneamino)nicotinonitrile (**2L**)

Yellow solid; yield: 77%. *Rf*=0.4 (4:1 hexane–EtOAc); mp: 115.4–116.3°C. ¹H-NMR (400 MHz, DMSO-*d*₆) δ: 9.05 (s, 1H), 8.48 (ddd, *J*=4.8, 1.9, 0.8 Hz, 1H), 7.88 (dd, *J*=1.8, 1.2 Hz, 1H), 7.61 (s, 1H), 7.33–7.31 (m, 1H), 7.13–7.06 (m, 1H), 6.45 (ddd, *J*=7.1, 5.0, 1.0 Hz, 1H), 4.29–4.16 (m, 4H), 2.22 - 2.10 (m, 2H). ¹³C-NMR (101 MHz, DMSO-*d*₆) δ: 161.82, 160.23, 154.80, 151.43, 149.25, 148.17, 139.01, 137.36, 131.52, 125.35, 122.61, 119.93, 112.23, 70.87, 70.76, 31.41. MS (ESI): *m/z* 280.1 [M+H]⁺. *Anal.* Calcd for C₁₆H₁₃N₃O₂: C 68.81, H 4.69, N 15.05, O 11.46; Found: C 68.87, H 4.73, N 14.96, O 11.37.

(*E*)-4-Chloro-*N*-((3,4-dihydro-2*H*-benzo[*b*][1,4]dioxepin-7-yl)methylene)pyridin-2-amine (**2M**)

White solid; yield 92%. *Rf*=0.4 (4:1 hexane–EtOAc); mp: 105.8–106.4°C. ¹H-NMR (400 MHz, DMSO-*d*₆) δ: 9.03 (s, 1H), 8.46 (dd, *J*=4.3, 1.7 Hz, 1H), 7.63 (dd, *J*=6.9, 1.9 Hz, 2H), 7.11 (d, *J*=8.9 Hz, 1H), 6.66 (d, *J*=1.7 Hz, 1H), 6.61 (dd, *J*=5.5, 1.9 Hz, 1H), 4.23 (ddd, *J*=11.4, 8.4, 3.7 Hz, 4H), 2.22–2.12 (m, 2H). ¹³C-NMR (100 MHz, DMSO-*d*₆) δ: 163.50, 161.40, 155.14, 151.40, 150.56, 149.87, 144.77, 128.80, 125.64, 122.86, 119.30, 112.17, 70.88, 70.73, 31.32. MS (ESI): *m/z* 289.4 [M+H]⁺. *Anal.* Calcd for C₁₅H₁₃ClN₂O₂: C 62.40, H 4.54, Cl 12.28, N 9.70, O 11.08; Found: C 62.45, H 4.57, Cl 12.23, N 9.68, O 11.12.

(*E*)-*N*-((3,4-Dihydro-2*H*-benzo[*b*][1,4]dioxepin-7-yl)-methylene)-4-methylpyridin-2-amine (**2N**)

White solid; yield: 88%. *Rf*=0.5 (4:1 hexane–EtOAc); mp: 153.3–153.6°C. ¹H-NMR (400 MHz, DMSO-*d*₆) δ: 9.05 (s, 1H), 8.33 (d, *J*=5.0 Hz, 1H), 7.75 (d, *J*=5.2 Hz, 1H), 7.61 (dd, *J*=6.9, 1.9 Hz, 2H), 7.18–7.03 (m, 1H), 6.31 (d, *J*=5.2 Hz, 1H), 4.23 (dt, *J*=13.6, 5.6 Hz, 4H), 2.36 (s, 3H), 2.15 (dd, *J*=11.2, 5.6 Hz, 2H). ¹³C-NMR (100 MHz, DMSO-*d*₆) δ: 161.60, 160.33, 154.73, 151.43, 149.79, 148.85, 147.84, 131.59, 125.27, 122.51, 120.50, 113.81, 70.86, 70.74, 31.42, 21.01. MS (ESI): *m/z* 269.2 [M+H]⁺. *Anal.* Calcd for C₁₅H₁₆N₂O₂: C 71.62, H 6.01, N 10.44, O 11.93; Found: C 71.68, H 6.11, N 10.39, O 11.88.

(*E*)-*N*-((3,4-Dihydro-2*H*-benzo[*b*][1,4]dioxepin-7-yl)-methylene)-3-methylpyridin-2-amine (**2O**)

White solid; yield: 86%. *Rf*=0.5 (4:1 hexane–EtOAc); mp: 145.8–146.1°C. ¹H-NMR (400 MHz, DMSO-*d*₆) δ: 8.99 (s, 1H), 8.32–8.23 (m, 1H), 7.68 (ddd, *J*=7.4, 1.7, 0.7 Hz, 1H), 7.65–7.59 (m, 2H), 7.19 (dd, *J*=7.4, 4.8 Hz, 1H), 7.12 (dd, *J*=12.7, 8.2 Hz, 1H), 4.24–4.16 (m, 4H), 2.38 (s, 3H), 2.16 (dd, *J*=5.7, 3.3 Hz, 2H). ¹³C-NMR (100 MHz, DMSO-*d*₆) δ: 160.74, 156.70, 151.47, 151.33, 146.54, 145.49, 139.47, 137.33, 132.28, 125.41,

122.50, 112.80, 70.88, 70.84, 30.96, 17.53. MS (ESI): m/z 269.2 $[M+H]^+$. Anal. Calcd for $C_{15}H_{16}N_2O_2$: C 71.62, H 6.01, N 10.44, O 11.93; Found: C 71.70, H 5.97, N 10.48, O 11.87.

Biology Bacterial suppressive assay: The antibacterial activity of the synthesized compounds was tested against *E. coli* ATCC 25922, *P. aeruginosa* ATCC 27853, *S. aureus* ATCC 6538 and *B. subtilis* ATCC 530 (kindly provided by pro Chang-Hong Liu, State Key Laboratory of Pharmaceutical Biotechnology, Nanjing University, Nanjing, China) using Mueller–Hinton medium (MH medium: 17.5 g casein hydrolysate, 1.5 g soluble starch, 1000 mL beef extract). The MIC values of the tested compounds were determined by a colorimetric method using MTT. A stock solution of the test compound (100 μ g/mL) in DMSO was prepared, and graded quantities were added to a specified volume of sterilized liquid MH medium. A specified volume of the compound-containing medium was then poured into microtiter plates. A suspension of the microorganism was prepared to contain approx. 105 cfu/mL and applied to microtiter plates with serially diluted compounds in DMSO to be tested and incubated at 37°C for 24 h. After the MIC values were visually determined on each of the microtiter plates, phosphate buffered saline (PBS; 50 μ L, 0.01 M, pH 7.4; 2.9 g $Na_2HPO_4 \cdot 12H_2O$, 0.2 g KH_2PO_4 , 8.0 g NaCl, 0.2 g KCl, 1000 mL distilled H_2O) containing MTT (2 mg/mL) was added to each well. Incubation was continued at RT for 4–5 h. The content of each well was removed, and 100 mL of isopropanol containing 5% HCl (final concentration 1 M) was added to extract the dye. After 12 h of incubation at RT, the optical density (OD) was measured with a microplate reader at 550 nm.

E. coli FabH inhibitory assay: Native *E. coli* FabH protein was overexpressed in *E. coli* DH10B cells using the pET30 vector (pET30 vector was kindly supplied by the State Key Laboratory of Pharmaceutical Biotechnology, Nanjing University) and purified to homogeneity in three chromatographic steps (Q-Sepharose, MonoQ, and hydroxyapatite) at 4°C. The selenomethionine-substituted protein was expressed in *E. coli* BL21(DE3) cells and purified in a similar way. Harvested cells containing FabH were lysed by sonication in 20 mM Tris (pH 7.6) containing 5 mM imidazole and 0.5 M NaCl, and centrifuged (20000 rpm, 30 min, 4°C). The supernatant was applied to a Ni-NTA agarose column, washed, and eluted using a 5–500 mM imidazole gradient over 20 column volumes. Eluted protein was dialyzed against 20 mM Tris (pH 7.6) containing 1 mM dithiothreitol (DTT) and 100 mM NaCl. Purified FabHs were concentrated to 2 mg/mL and stored at –80°C in 20 mM Tris (pH 7.6) containing 100 mM NaCl, 1 mM DTT, and 20% glycerol for enzymatic assay.

In a final 20 μ L reaction, 20 mM Na_2HPO_4 (pH 7.0) containing 0.5 mM DTT, 0.25 mM $MgCl_2$, and 2.5 μ M holo-ACP were mixed with 1 nM FabH, and H_2O was added to 15 μ L. After 1 min incubation, a 2 μ L mixture of 25 μ M acetyl-CoA, 0.5 mM reduced nicotinamide adenine dinucleotide (NADH), and 0.5 mM reduced nicotinamide adenine dinucleotide phosphate (NADPH) was added for FabH reaction for 25 min. The reaction was stopped by adding 20 μ L of ice-cold 50% trichloroacetic acid (TCA), incubating for 5 min on ice, and centrifuging to pellet the protein. The pellet was washed with 10% ice-cold TCA and resuspended in 0.5 M NaOH (5 μ L). The incorporation of the 3H signal in the final product was read by liquid scintillation. When determining the IC_{50} values, inhibi-

tors were added from a concentrated DMSO stock such that the final concentration of DMSO did not exceed 2%.

Cytotoxicity test: The cytotoxic activity *in vitro* was measured against mouse fibroblast NIH-3T3 cells using the MTT assay. Cells were cultured in a 96-well plate at a density of 5×10^{-5} cells and different concentrations of compounds were respectively added to each well. The incubation was permitted at 37°C, 5% CO_2 atmosphere for 24 h before the cytotoxicity assessments. Twenty microliters MTT reagent (4 mg/mL) was added per well 4 h before the end of the incubation. Four hours later, the plate was centrifuged at 1200 rcf for 5 min and the supernatants were removed, each well was added with 200 μ L DMSO. The absorbance was measured at a wavelength of 570 nm (OD570 nm) on an enzyme-linked immunosorbent assay (ELISA) microplate reader. Three replicate wells were used for each concentration and each assay was measured three times, after which the average of IC_{50} was calculated. The cytotoxicity of each compound was expressed as the concentration of compound that reduced cell viability to 50% (IC_{50}).

Docking Study Molecular docking of compound 2E into the 3D Xray structure of *E. coli* FabH (PDB: 1HNJ)⁸ was carried out using Discovery Studio (v3.1) as implemented through the graphical user interface DS-CDOCKER protocol.²¹

The 3D structures of the aforementioned compounds were constructed using Chem 3D ultra 12.0 (Chemical Structure Drawing Standard; Cambridge Soft Corporation, U.S.A.) and energy minimized by using MMFF94 with 5000 iterations and minimum RMS gradient of 0.10. The crystal structures of *E. coli* FabH (PDB: 1HNJ)⁸ complex were retrieved from the RCSB Protein Data Bank (<http://www.rcsb.org/pdb/>). All bound waters and ligands were eliminated from the protein and the polar hydrogen was added to the proteins.

Acknowledgment This work was financed by China Postdoctoral Science Foundation.

Conflict of Interest The authors declare no conflict of interest.

References

- 1) Abraham E. P., "Discovery and Development of Penicillin." The Dent Record, London, 1946, pp. 197–200.
- 2) Walsh C., *Nat. Rev. Microbiol.*, **1**, 65–70 (2003).
- 3) Lai C. Y., Cronan J. E., *J. Biol. Chem.*, **278**, 51494–51503 (2003).
- 4) Lu Y. J., Zhang Y. M., Rock C. O., *Biochem. Cell Biol.*, **82**, 145–155 (2004).
- 5) Natarajan S., Kim J. K., Jung T. K., Doan T. T., Ngo H. P., Hong M. K., Kim S., Tan V. P., Ahn S. J., Lee S. H., Han Y., Ahn Y. J., Kang L. W., *Mol. Cells*, **33**, 19–25 (2012).
- 6) Payne D. J., Warren P. V., Holmes D. J., Ji Y., Lonsdale J. T., *Drug Discov. Today*, **6**, 537–544 (2001).
- 7) Heath R. J., White S. W., Rock C. O., *Prog. Lipid Res.*, **40**, 467–497 (2001).
- 8) Raman K., Rajagopalan P., Chandra N., *PLOS Comput. Biol.*, **1**, e46 (2005).
- 9) Li H. Q., Luo Y., Zhu H. L., *Bioorg. Med. Chem.*, **19**, 4454–4459 (2011).
- 10) Wang Y., Ma S., *ChemMedChem*, **8**, 1589–1608 (2013).
- 11) Heath R. J., Rock C. O., *J. Biol. Chem.*, **271**, 1833–1836 (1996).
- 12) Revill W. P., Bibb M. J., Scheu A. K., Kieser H. J., Hopwood D. A., *J. Bacteriol.*, **183**, 3526–3530 (2001).

- 13) Qiu X., Janson C. A., Smith W. W., Head M., Lonsdale J., Konstantinidis A. K., *J. Mol. Biol.*, **307**, 341–356 (2001).
- 14) Khandekar S. S., Konstantinidis A. K., Silverman C., Janson C. A., McNulty D. E., Nwagwu S., Van Aller G. S., Doyle M. L., Kane J. F., Qiu X., Lonsdale J., *Biochem. Biophys. Res. Commun.*, **270**, 100–107 (2000).
- 15) Davies C., Heath R. J., White S. W., Rock C. O., *Structure*, **8**, 185–195 (2000).
- 16) Nie Z., Perretta C., Lu J., Su Y., Margosiak S., Gajiwala K. S., Cortez J., Nikulin V., Yager K. M., Appelt K., Chu S. S., *J. Med. Chem.*, **48**, 1596–1609 (2005).
- 17) Ashek A., San-Juan A. A., Cho S. J., *J. Enzyme Inhib. Med. Chem.*, **22**, 7–14 (2007).
- 18) Lai C. Y., Cronan J. E., *J. Biol. Chem.*, **278**, 51494–51503 (2003).
- 19) He X., Reeve A. M., Desai U. R., Kelloqq G. E., Reynolds K. A., *Antimicrob. Agents Chemother.*, **48**, 3093–3102 (2004).
- 20) Lee J. Y., Jeong K. W., Lee J. U., Kang D. I., Kim Y., *Bioorg. Med. Chem.*, **17**, 1506–1513 (2009).
- 21) Jones P. B., Parrish N. M., Houston T. A., Stapon A., Bansal N. P., Dick J. D., Townsend C. A., *J. Med. Chem.*, **43**, 3304–3314 (2000).
- 22) Khandekar S. S., Gentry D. R., Van Aller G. S., Warren P., Xiang H., Silverman C., Doyle M. L., Chambers P. A., Konstantinidis A. K., Brandt M., Daines R. A., Lonsdale J. T., *J. Biol. Chem.*, **276**, 30024–30030 (2001).
- 23) Li Y., Zhao C. P., Ma H. P., Zhao M. Y., Xue Y. R., Wang X. M., Zhu H. L., *Bioorg. Med. Chem.*, **21**, 3120–3126 (2013).
- 24) Lv P. C., Wang K. R., Yang Y., Mao W. J., Chen J., Xiong J., Zhu H. L., *Bioorg. Med. Chem. Lett.*, **19**, 6750–6754 (2009).
- 25) Zhou Y., Du Q. R., Sun J., Li J. R., Fang F., Li D. D., Qian Y., Gong H. B., Zhao J., Zhu H. L., *ChemMedChem*, **8**, 433–441 (2013).
- 26) Discovery Studio 3.1, Accelrys Software Inc., San Diego, CA, 2011.
- 27) Ertl P., Rohde B., Selzer P., *J. Med. Chem.*, **43**, 3714–3717 (2000).
- 28) Lee J. Y., Jeong K. W., Shin S., Lee J. U., Kim Y., *Eur. J. Med. Chem.*, **47**, 261–269 (2012).